ELSEVIER

Prenylated flavonoids from *Dalea* genus as xanthine oxidase inhibitors: *In vitro* bioactivity evaluation and molecular docking studies

M.D. Santi [a], E. Bedoya Aguirre [a,b], M.F. Negro [a,b], M. Paulino Zunini [c], M.A. Peralta [a,b], M. G. Ortega [a,b,*]

[a] *Instituto Multidisciplinario de Biología Vegetal (IMBIV-CONICET), Ciudad Universitaria. X5000HUA Córdoba, Argentina*
[b] *Farmacognosia, Departamento de Ciencias Farmacéuticas, Facultad de Ciencias Químicas, Universidad Nacional de Córdoba, Ciudad Universitaria, Haya de la Torre y Medina Allende, Edificio Ciencias II, X5000HUA Córdoba, Argentina*
[c] *Área Bioinformática, DETEMA, Facultad de Química, Universidad de la República, 11800 Montevideo, Uruguay*

ARTICLE INFO

ABSTRACT

Prenylated flavanones are a family of compounds with an important biological potential. Previously, anti-tyrosinase activity, acetylcholinesterase inhibitory activity, and neuroprotective effects of several prenyl flava-nones isolated from different American *Dalea* genus species were reported. The biological potency of these kinds of compounds, together with the particularity of their chemical structures, encouraged us to investigate them for *in vitro* and *in silico* anti-xanthine oxidase activity. So, five prenyl-flavanones obtained from different *Dalea* sp (*Dalea elegans*, *Dalea boliviana*, and *Dalea pazensis*) were studied and the relationships between the structure of these prenyl-flavanones and their inhibitory activity were evaluated. Molecular docking studies were performed in order to propose the binding mode of the most active natural compound. 2′,4′-dihydroxy-5′-(1‴,1‴-dimethy-lallyl)-8-prenylpinocembrin (1) was the most active in this series showing an IC$_{50}$ of 0.26 ± 0.07 μM comparable with the reference inhibitor, allopurinol. The presence of 5,7,2′,4′-tetrahydroxy substitution, accompanied by a prenyl group at 8-position in the A-ring, and a 5′ (1‴,1‴-dimethylallyl) were important to present a xanthine oxidase inhibitory activity. This fact was confirmed with molecular docking studies showing relevant interactions of 1 with the residues of the catalytic site of xanthine oxidase, and a binding energy of −7.3297 kcal mol^{-1}. These results contributed not only to understanding the binding mode but also to validating the *in vitro* results. The obtained findings lead us to propose these prenyl-flavanones as lead compounds for the design and devel-opment of novel xanthine oxidase inhibitors for the treatment of diseases in which this enzyme is involved.

Introduction

Xanthine oxidase (XO, EC 1.17.3.2) is a key metalloenzyme in purine metabolism. It is responsible for the conversion of hypoxanthine to xanthine and finally, the synthesis of uric acid, which is produced by reactive oxygen species as products of those reactions [1–3]. During pathological states, the generated hyperuricemia is considered a relevant risk factor for developing nephrolithiasis, gout, hypertension, cardiovascular diseases, diabetes, and oxidative damage in tissues [4,5]. For that reason, the inhibition of XO is a relevant pharmacological target, not only for hyperuricemia treatment. Allopurinol (AL) and oxypurinol, both recognized XO inhibitors, have shown side effects, such as hepatitis, nephropathy, and skin rash [6–8]. Therefore, the search for new XO inhibitors is imperative. Focusing in that direction, it is

recognized the relevant activity of flavonoids as XO inhibitors [2,5,7,8–11]. Several studies reported the structural-activity relationship (SAR) for that kind of compound, showing the influence of the substitution pattern of phenol/hydroxyl groups on the XO inhibitory activity [2,7,8]. Recently, we demonstrated the influence of methoxyl substituents in the A and B rings of different natural and semisynthetic flavonoids from *Gardenia oudiepe* Vieill. [12]. Few studies have evaluated other structural requirements such as the presence of a prenyl moiety [13,14].

Dalea L (Fabaceae) is an American genus with a distribution from the southwestern United States to central Argentina and Chile. It was widely demonstrated that this genus is rich in flavonoid content with relevant biological activities [15]. Particularly, some species from this genus present relevant chemical content in prenylated flavonoids. This family

of compounds is considered "rare" due to their low natural abundance in the plant kingdom. They have shown interesting biological activities, such as antimicrobial, inhibition of resistance mechanisms in bacteria and fungi, inhibition of tyrosinase enzyme and acetylcholinesterase enzyme, as well as, neuroprotection [15,16]. Previously, we have reported the isolation and characterization of several prenylated flavanones (PFs) from *Dalea elegans* Gillies ex Hook. et Arn, *Dalea boliviana* Britton and *Dalea pazensis* Rusby. All of them were evaluated as mushroom tyrosinase inhibitors, and the most active were proposed as important candidates for the development of hyperpigmentary disorders' treatments [15,17–20]. Furthermore, we have previously shown that some of them presented protective effects against oxidative stress-induced death in two *in vitro* models of neurodegenerative diseases, as well as acetylcholinesterase inhibitory activity [16].

In relation to the above presented, and taking into account the biological potential of that family of compounds, this work aimed at the evaluation of the *in vitro* XO inhibitory activity of five PFs obtained from *D. elegans, D. boliviana, and D. pazensis*. In addition, and with the objective of establishing SAR, the XO inhibitory activity of the commercial flavanone pinocembrin was measured. Our results present for the first time, natural prenylated flavonoids as lead molecules for the rational development of therapeutic strategies for hyperuricemia treatment and prevention.

Materials and methods

Plant material

D. elegans (Fabaceae) was collected in February 2012, in the flowering period, near Cabalango (Córdoba, Argentina, GPS coordinates: latitude: 31°24′ 04.62″ South; longitude: 64°34′19.21″ West; height: 763 m). Prof. Dr. Gloria Barboza from the Botanical Museum, Universidad Nacional de Córdoba, Argentina (CORD), identified it. A voucher specimen was deposited as CORD Peralta 2.

D. boliviana Britton (Fabaceae) was collected in February 2019, at Iturbe in the Humahuaca Department, Jujuy province, Argentina (GPS coordinates 22°58′44″ S, 65°21′13″ W at 3223 m above sea level). A voucher specimen was deposited as CORD 1066 in the Botanical Museum, Universidad Nacional de Córdoba, Argentina. The Plant material was identified by Prof. Dr. Gloria Barboza of the Museo Botánico-UNC.

Roots of *D. pazensis* Rusby (Fabaceae) were collected in March 2013, in Yotala, a locality close to Sucre city (19°08′53″ s 65°15′48″ W at 2543 m above sea level). A voucher specimen was identified by specialized personnel from the Herbario del Sur de Bolivia (HSB) (Portal E. & Lopez C.C.) and deposited as 961A.

Isolation, purification, and identification

(2S)-2′,4′-dihydroxy-5′-(1‴,1‴-dimethylallyl)-8-prenylpinocembrin (8PP, **1**) and (2S)-8-prenylpinocembrin (8P, **2**) were obtained from *D. elegans* roots and aerial parts, respectively and identified as previously described by Peralta et al. (2014) [19]. (2S)-5,7,2′-trihydroxy-5′-(1‴,1‴-dimethylallyl)-8-prenylflavanone (**3**) and (2S)-5,7,2′-trihydroxy-8,3′-diprenylflavanone (**4**) were obtained from roots of *D. boliviana* and their identification was according with Peralta et al. (2011) [18]. (2S)-3′,4′-dihydroxy-6,2′-diprenylpinocembrin (pazentin A, **5**) was isolated from roots of *D. pazensis* as previously informed by Santi et al. (2017) [20]. Briefly, roots or aerial parts were dried at room temperature, powered, and processed for extraction and isolation of the natural compounds as we previously reported, by using the soxhlet technique, column chromatography, and preparative TLC. Their identification was performed by comparing their HRMS, NMR spectroscopic data, UV absorption profiles, and Circular Dichroism with our previously isolated compounds as references.

Compound **1** was isolated as a yellow amorphous solid; UV (MeOH) λ_{max} (log ε) 294 (3.49), 334 (sh) (2.91) nm; CD (c 0.162, MeOH) [θ]$_{294}$–0.31, [θ]$_{334}$ + 0.18. For ^{1}H NMR (CDCl$_3$, 400 MHz) and ^{13}C NMR (CDCl$_3$,100 MHz) data, please refer to Peralta et al. (2014) [19]. HRMS m/z 423.1834 [M − H]$^-$ (calculated for C$_{25}$H$_{27}$O$_6$, 423.1802).

Compound **2** was isolated as a white amorphous solid; UV (MeOH) λ_{max} (log ε) 294 (4.91), 334 (sh) (4.33) nm; CD (c 0.006, MeOH) [θ]$_{294}$–2.67, [θ]$_{334}$ + 0.35. For ^{1}H NMR (CDCl$_3$, 400 MHz) and ^{13}C NMR (CDCl$_3$, 100 MHz) data, please refer to Peralta et al. (2014) [19]. HRMS m/z 323.1292 [M − H]$^-$ (calculated for C$_{20}$H$_{19}$O$_4$, 323.1278).

Compound **3** was isolated as an amorphous solid; UV (MeOH) λ_{max} (log ε) 293 (4.09), 339 (sh) (3.44) nm; CD (c 0.098, MeOH,) [θ]$_{293}$–36.68, [θ]$_{334}$ + 2.33; IR (KBr) ν_{max} 3389 (OH), 2962, 2921,1637 (C=O), 1601, 1506 (C=C), 1270 cm^{-1}. For ^{1}H NMR (acetone-d_6, 400 MHz) and ^{13}C NMR (acetone-d_6,100 MHz) data, please refer to Peralta et al. (2011) [18]. HRFABMS m/z 409.2016 [M + H]$^+$ (calculated for C$_{25}$H$_{29}$O$_5$, 409.2015).

Compound **4** was obtained as a yellow amorphous solid; UV (MeOH) λ_{max} (log ε) 274 (sh) (1.98), 293 (2.09), 339 (sh) (1.45) nm; CD (c 0.049, MeOH) [θ]$_{290}$–41.05, [θ]$_{340}$ + 2.47; IR (KBr) ν_{max} 3446 (OH), 1631 (C=O), 1542 (C=C), 1446 cm^{-1}; ^{1}H NMR (CDCl$_3$, 400 MHz) and ^{13}C NMR (CDCl$_3$, 100 MHz), data please to Peralta et al. (2011) [18]; HRFABMS m/z 409.2009 [M + H]$^+$ (calculated for C$_{25}$H$_{29}$O$_5$, 409.2015).

Compound **5** was isolated as a yellow amorphous solid; UV (MeOH) λ_{max} (log ε) 293 (3.69), 330 (sh) (3.13) nm; CD (c 0.004, MeOH) [θ]$_{293}$–0.46, [θ]$_{330}$ + 0.05; IR (KBr) ν_{max} 3644, (OH), 2921, 1644 (C=O), 1601, 1455 (C=C) 2852 (OCH$_3$), cm^{-1}. For ^{1}H NMR (acetone-d_6, 400 MHz) and ^{13}C NMR (acetone-d_6, 100 MHz) data, please refer to Santi et al. (2017) [20]. HRMS m/z 447.1775 [M$^+$Na]$^+$ (calculate for C$_{25}$H$_{27}$O$_6$, 447.1778).

Chemicals

XO (EC 1.17.3.2) from bovine milk (0.04 U/mL), allopurinol (AL; purity: 99%), Xanthine (purity: 99,5%), HCl (1 N), and pinocembrin (**6**, purity: 95%) were obtained from Sigma Chemical Co. (St. Louis, MO, USA). All the solvents employed presented an analytical grade.

In vitro XO inhibitory activity

The assay was realized as earlier described by Schmeda-Hirschmann et al., 1992 [21]. Briefly, 21.4 μL of XO solution and 0.75 mL of the control solution [K$_2$HPO$_4$/KH$_2$PO$_4$ buffer (0.07 M, pH 7.5)] or the sample solution [constituted by each PF or AL dissolved in dimethylsulfoxyde (DMSO; final concentration of 0.1% v/v) and subsequently diluted to the adequate concentrations with the above buffer] were combined and pre-incubated at 25 °C for 15 min. That step involves a pre-treatment of the enzyme with either the control solution or the natural compounds to be evaluated allowing the equilibrium before the reaction is started according to the reference [21]. Then [22,23,24], 0.45 mL of the substrate (xanthine solution, 150 mM) was added, and incubated at 25 °C for 30 min, time needed to ensure an adequate enzymatic process according to the previously calculated by Schmeda-Hirschmann et al., 1992 [21] and validated by us [12]. By the addition of 1 mL of HCl (1 N), the reaction was stopped [25] according to Schmeda-Hirschmann et al., 1992 [21], and the absorbance was measured at 290 nm on a Cary Win UV–VIS spectrophotometer, Varian, Inc. Agilent Technologies (Santa Clara, USA). The positive inhibitor control was AL. The percent inhibition of XO activity was calculated as follows: % inhibition = [(Abs$_{control}$ - Abs$_{sample}$)/Abs$_{control}$] × 100, where Abs$_{control}$ is the absorbance of the control solution and Abs$_{sample}$ is the absorbance of the sample solution.

Calculations and statistics

The biological assays were performed in triplicate, and the results

were expressed as media ± SD of three separate experiments. The values of the IC$_{50}$ were estimated by the *GraphPad Prism* 6.0 software on a compatible computer. The unidirectional analysis of variance (ANOVA) followed by Bonferroni's test for multiple comparisons of the results was realized using *GraphPad Prism* 6.0 software.

Molecular docking studies

Molecular docking studies were performed by using the coordinates of the milk bovine XO 3D structure deposited at the Protein Data Bank (https://www.rcsb.org/pdb; PDB ID 3NVY), co-crystallized with quercetin, solved at 2.0 Å resolution [26]. We processed the crystallographic coordinates and ran our studies on MOE™ suite (Chemical Computing Group Inc. https://www.chemcomp.com) [27], as we previously reported [12,15]. Briefly, 3NVY crystal was processed and water molecules were deleted since they were not essential to the interaction under study. Through the MMFF94 forcefield, hydrogen atoms and charges were adjusted, and 3D structures of all isolated and structurally identified PFs and pinocembrin were built and minimized [28,29]. Different conformers were generated with the conformational search LowmodeMD [30] on the fly in the molecular docking procedure. Residues within a 4.5 Å sphere centered on quercetin atoms were taking account for the docking experiments. Triangle Matcher was selected as a placement function and scores were calculated with the Affinity DG function (MOE™ Chemical Computing Group, 2009) [27]. We have validated our study, by reproducing the same pose of quercetin inside the active site, with a 2.8 Å root mean square deviation (RMSD) [12,31,32]. Surface Maps and Ligand Interaction MOE™ tools were used to generate graphical representations of resulting complexes XO-flavonoid.

Results and discussion

Prenylflavanones XO inhibitory activities

In this study, five PFs: 8PP (**1**), 8P (**2**), **3**, **4**, and pazentin A (**5**) (Fig. 1) isolated from *Dalea* species (*D. elegans, D. boliviana, and D.*

pazensis), together with the commercially available flavonoid pinocembrin (**6**), were evaluated for their XO inhibitory activity.

All flavanones showed a concentration-dependent inhibition. The IC$_{50}$ values for **1**–**6** and the reference inhibitor AL were estimated using nonlinear fitting of concentration–response (Table 1).

As a result, **1** was the most active of this series, and showed a similar activity (not significative different, t student test, p-value: 0.6594) with respect to the reference inhibitor AL (Fig. 2). It is important to highlight that we have previously reported the cytotoxicity of compound 1, the most active compound of these series, on B16F0 melanoma cells [20]. The maximum non-cytotoxic concentration (MNCC) was estimated to be (10.0 ± 1.0 μM). This result supports the fact that compound **1** does not show cytotoxic effects on B16F0 at the concentration at which it was observed a 50% inhibition on XO (0.26 ± 0.07 μM). However, further studies should be performed, such as an evaluation of cytotoxicity in other cell lines, to ensure its safety and later translate this result to clinical use.

Structure-activity relationships

Former reports highlighted some structural requirements as the presence of hydroxy groups in positions 5, 7, and 4′ of flavones [2,7,8]. Recently, we incorporated information about methoxy substitutions

Table 1
Estimated IC$_{50}$ values corresponding to XO inhibitory activity of flavanones **1**–**6** and the reference inhibitor AL.

Compound	IC$_{50}$ (μM)
1	0.26 ± 0.07
3	0.69 ± 0.03
4	2.5 ± 0.5
2	3.9 ± 0.8
6	12.0 ± 0.7
5	ND (13.8% at 100 μM)
AL	0.247 ± 0.004

ND: Not determined.
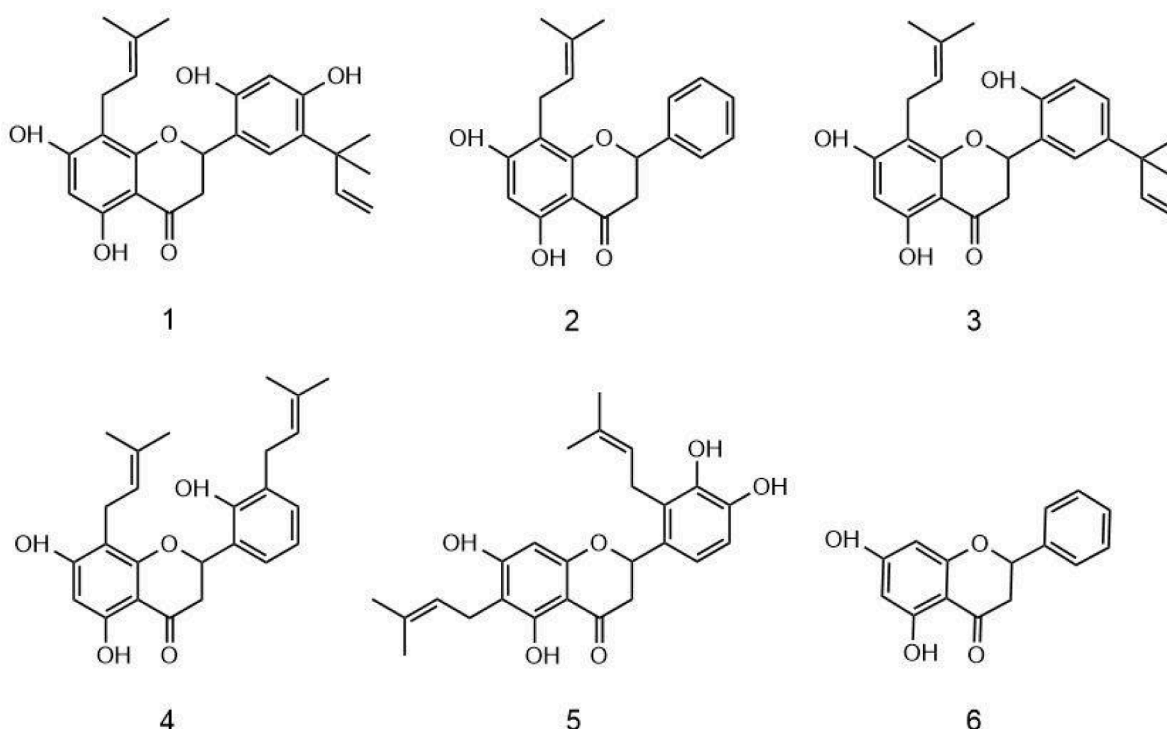
Fig. 1. Structures of prenylated flavanones isolated from *Dalea* species (**1**–**5**) and pinocembrin (**6**).
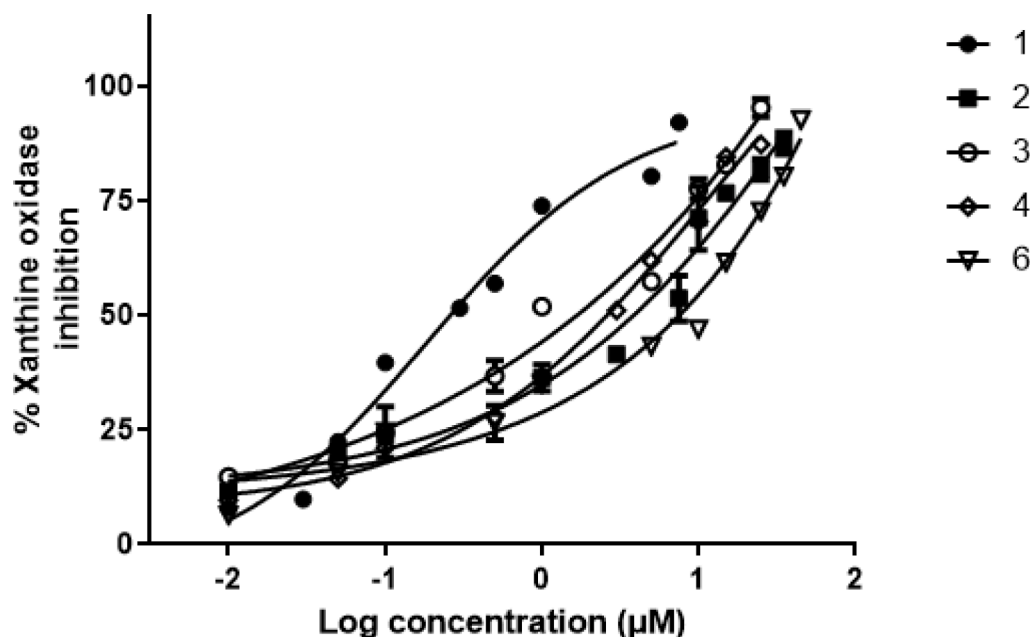
Fig. 2. IC_{50} profiles of prenylated flavanones **1**–**4** and **pinocembrin (6)**.

[20].

The present work extends these data to flavanones bearing a combination of prenyl and hydroxy substitutions, which were, to our knowledge, never evaluated for their *in vitro* XO inhibitory activity.

The majority of the prenylflavanones tested (**1**–**4**) share a core including a 5, 7-dihydroxy and 8-prenyl moiety in A-ring, but compound **5** differs in that the prenyl moiety is positioned in 6 (Fig. 1). Regarding the B-ring, the variability in these prenylflavanones is due to the presence/absence of prenyl or dimethylallyl, and hydroxyl substituents in different positions of the ring. So, it is important to elucidate how the different patterns of substitution are influencing the XO inhibitory activity observed in this series. Compound **1** has been identified as the most active within this series, showing an IC_{50} of 0.26 ± 0.07 μM. Moreover, we incorporated 5,7-dihydroxyflavanone (pinocembrin, **6**), to determine relevant structural requirements for activity, and it turned out to be the one with the lowest activity (IC_{50} 12.0 ± 0.7 μM), compared to the active compounds. These findings reinforce the relevance of substitution in B-ring and the presence of 8-prenyl moiety in A-ring. Another relevant structural requirement is the presence of 2′, 4′-dihydroxy in B-ring next to prenyl moiety in 5′. In compounds **2**, **3**, and **4**, where the structural pattern in the B-ring is different to compound **1**, the inhibitory activity of XO decreases almost 3, 10, and 15-fold respectively compared with **1**, showing the relevance of the presence of the pattern above mentioned for B-ring. On the other hand, interestingly we found that the PF isolated from *D. pazensis* (**5**) was inactive. This compound does not present the B-ring pattern that we showed as relevant to present XO inhibitory activity. Furthermore, its prenyl group at A-ring is in position 6, instead of position 8, leading us to confirm the importance of 8-prenyl moiety in the A-ring to show inhibitory activity. Taking all those facts together, we could affirm that a 5, 7, 2′, 4′-tetrahydroxy substitution, accompanied by a prenyl group at 8-position in the A-ring and a 5′-(1‴,1‴-dimethylallyl) are important chemical features to present an XO inhibitory activity comparable to the inhibitor of reference AL. Remarkably, the observed chemical structural conditions to present XO inhibitory activity are shared with those shown by the same PFs to present inhibitory activity on tyrosinase enzyme [19,20]. Furthermore, compounds **1** and **2** have also shown neuroprotective activity on neurons after oxidative injury, and the same mentioned substitution pattern was observed to lead to the most potent flavanones [16]. This multi-target behavior could be exploited in the development

of new pharmacological strategies to prevent and/or treat pathologies with increased oxidative stress, such as neurodegenerative diseases, melanoma, and gout.

In silico molecular docking studies

In order to understand the binding mode between the most active compound of the series (**1**) and XO (PDB ID: 3NVY) [26], we carried out computational docking studies by using the MOE^TM tool (2014) [27]. As we previously described, a sphere of 4.5 Å around the co-crystallized ligand (quercetin), including essential amino acids was selected as "docking site" [33] (Fig. 3).

PF **1** showed important interactions between B-ring substituents (OH and dimethylallyl substituents) and residues of the catalytic XO active site, such as Glut802 and Phe914 or Glut802 which has an essential role in the XO substrate hydroxylation (xanthine) [33], while Phe914 was reported as important for the recognition of the ligand by XO (Fig. 4).

The binding energy of **1** was −7.3297 kcal mol⁻¹, being the lowest of the series. For the rest of the compounds, we found binding energies of: −5.3429 (**3**), −5.2264 (**4**), −5.2107 (**8P, 2**), −5.1038 (**pinocembrin, 6**), −5.1464 (**pazentin A, 5**) kcal/mol. These results were in concordance with those obtained on *in vitro* assays (Table 1).

In Fig. 5, a 2D graphic description of the ligand interactions are shown. As can be seen, PF **1** benzopyranone ring is sandwiched between Phe914 and Phe1009 residues and also presents a π-π interaction between the A ring and the aromatic ring of the Phe914 residue. This interaction, was previously reported as important for the recognition ligand-XO, and we hypothesize here that in this case, it could be enhanced thanks to the presence of the lipophilic prenyl substituent at position 8 of the A-ring, which is also presenting hydrophobic interactions with residues Leu873, Pro1076, Met1038 that belong to the XO active cavity. These interactions could prevent further binding XO-substrate (xanthine or hypoxanthine) stabilizing compound **1**-XO interaction [8,34,35].

Other hydrophobic interactions could be seen between the B-ring and residues Ala1078, and Ala1079, which also contribute to stabilizing the complex compound **1**-XO [36,37]. Moreover, we found important polar interactions with residues Glu802, Glu1261, Arg880, and Arg912 reported as crucial in the hydroxylation of substrate xanthine [9,11,13,38]. A hydrogen binding with Glu802 and OH-2′ is reinforcing
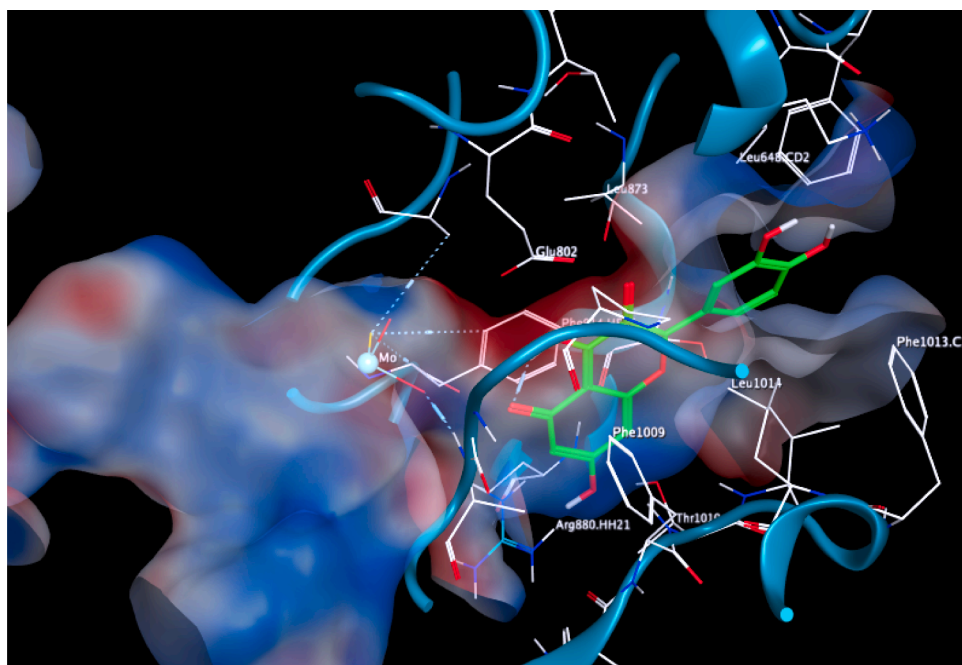
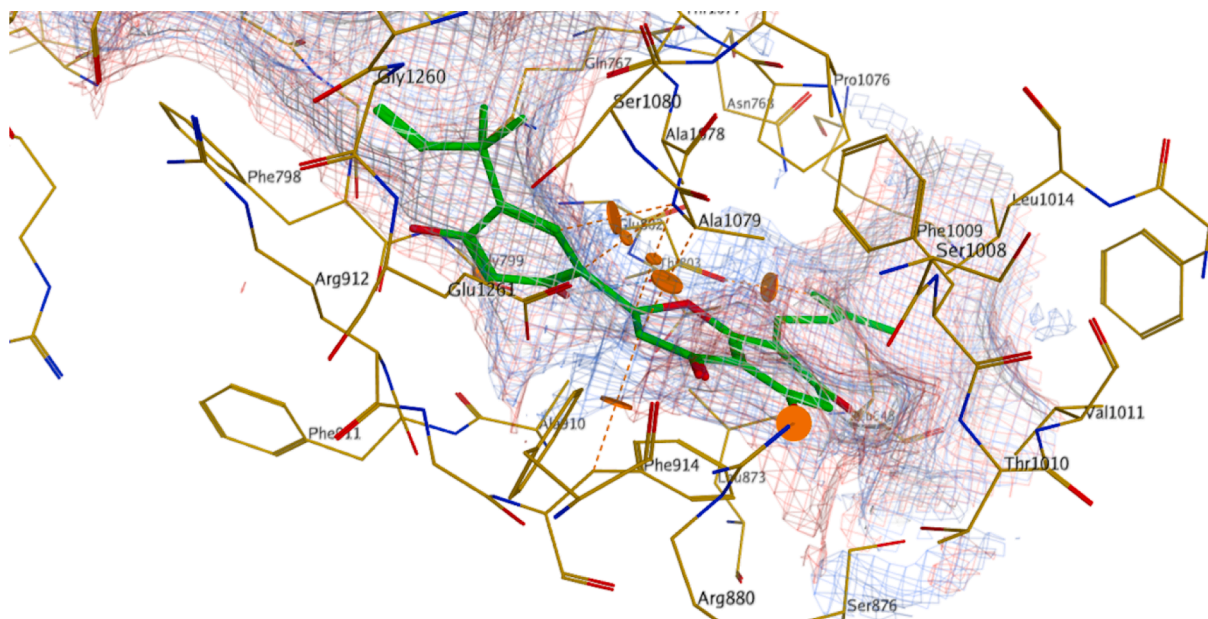**Fig. 3.** XO (3NVY) pocket with quercetin as co-crystallized ligand.

Fig. 4. PF **1** 2D Electrostatic Surface Map. It is shown the best pose docked of **1**. Blue color corresponds to electropositive surface areas, and red color is representing the negative electrostatic surfaces. (For interpretation of the references to color in this figure legend, the reader is referred to the web version of this article.)

the fact that OH in B-ring is important to assist the inhibitory activity [11]. Further studies should be performed as Molecular Dynamics to complete the evaluation for compound **1** in particular to consider the solvent and or flexibility influence. We also thought that it will be interesting to evaluate the effect of a combination of our prenyl-flavanones and AL. Although some of them were less active than AL, a combination could result in a potent synergism allowing diminishing the AL dose necessary to inhibit XO, and subsequently its adverse effects. *In vivo* studies could also help to confirm the bioactivity of these natural compounds on hyperuricemic models and go deeper into toxicity and bioavailability evaluations.

Conclusion

In this work, we presented the *in vitro* XO inhibition of five PFs isolated from *Dalea* genus. Compound **1** presented a similar activity with respect to the reference inhibitor, AL. Compound **3** was 3-fold less active than AL, and the other flavanones showed to be much less active (**4**, **6**), or inactive (**5**). Considering the biological potentiality of this kind of compounds, we propose to evaluate them in combination with AL, in order to test a possible synergic effect between them. Also, we are encouraged to say that the active PFs tested here, could be exploited as lead molecules for the rational design of new XO inhibitors.
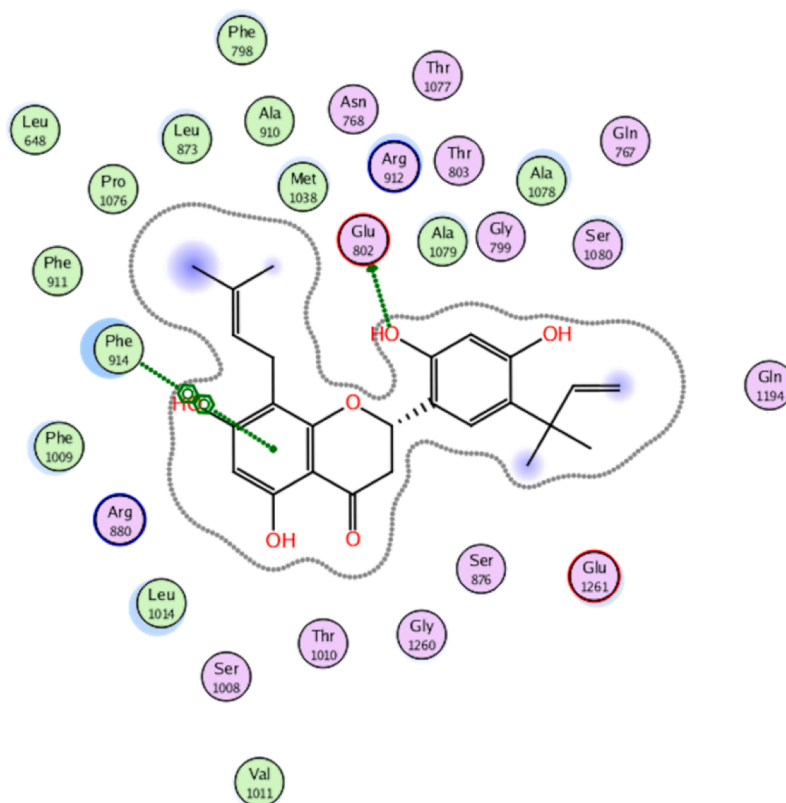
According to our knowledge, we inform for the first-time

Fig. 5. Ligand interaction of PF **1** and XO (3NVY) residues in the active site.

structure–activity relationships of PFs as XO inhibitors. Additionally, *in silico* studies of PF, **1** showed important interactions between the natural compound and amino acid residues of the XO active site. That fact not only confirms the obtained results in the *in vitro* evaluation but also suggests that the interaction between **1** and XO is stable and supported by multiple Van der Waals and hydrogen binding interactions. It is important to mention, that we have previously demonstrated that compound **1** does not present cytotoxic effects in B16F0 cells at the concentration in which present XO inhibition (~0.26 μM).

Our data allows us to propose PF **1** as a candidate for the treatment of disorders/diseases in which XO activity is exacerbated. Moreover, PF **1** has previously demonstrated not only inhibitory activity on tyrosinase enzyme, and acetylcholinesterase, but also neuroprotective effects against oxidative stress-induced death in different models of neurodegenerative diseases. All that data, led us to present PF **1** as a multi-target flavanone with the potential to be evaluated as a lead compound for the design and development of new pharmacological strategies for the prevention and treatment of pathologies with associated oxidative stress.

CRediT authorship contribution statement

M.D. Santi: Conceptualization, Methodology, Validation, Investigation, Data curation, Writing – original draft, Writing – review & editing. **E. Bedoya Aguirre:** Investigation. **M.F. Negro:** Investigation. **M. Paulino Zunini:** Methodology, Resources, Writing – review & editing. **M.A. Peralta:** Conceptualization, Resources, Methodology, Writing – review & editing, Funding acquisition. **M.G. Ortega:** Investigation, Supervision, Conceptualization, Resources, Methodology, Writing – review & editing, Project administration, Funding acquisition.

Declaration of Competing Interest

The authors declare that they have no known competing financial interests or personal relationships that could have appeared to influence the work reported in this paper.

Data availability

Data will be made available on request.

References

[1] Y.H. Chu, C.J. Chen, S.H. Wu, J.F. Hsieh, Inhibition of xanthine oxidase by rhodiola crenulata extracts and their phytochemicals, J. Agric. Food Chem. 62 (17) (2014) 3742–3749, https://doi.org/10.1021/jf5004094.

[2] D.E.C. Van Hoorn, R.J. Nijveldt, P.A.M. Van Leeuwen, Z. Hofman, L. M'Rabet, D.B. A. De Bont, K. Van Norren, Accurate prediction of xanthine oxidase inhibition based on the structure of flavonoids, Eur. J. Pharmacol. 451 (2) (2002) 111–118.

[3] H.-C. Lin, S.-H. Tsai, C.-S. Chen, Y.-C. Chang, C.-M. Lee, Z.-Y. Lai, C.-M. Lin, Structure-activity relationship of coumarin derivatives on xanthine oxidase-inhibiting and free radical-scavenging activities, Biochem. Pharmacol. 75 (2008) 1416–1425, https://doi.org/10.1016/j.bcp.2007.11.023. PMID: 18201686.

[4] J. Wang, S. Liu, B. Ma, L. Chen, F. Song, Z. Liu, C.M. Liu, Rapid screening and detection of XOD inhibitors from S. Tamariscina by ultrafiltration LC-PDA-ESI-MS

combined with HPCCC, Anal. Bioanal. Chem 406 (28) (2014) 7379–7387, https://doi.org/10.1007/s00216-014-8132-x. PMID: 25240932.

[5] A. Nagao, M. Seki, H. Kobayashi, Inhibition of xanthine oxidase by flavonoids, Biosci. Biotechnol. Biochem. 63 (10) (1999) 1787–1790, https://doi.org/10.1271/bbb.63.1787. PMID: 10671036.

[6] H.A. Jung, H.E. Moon, S.H. Oh, B.W. Kim, H.S. Sohn, J.S. Choi, Kinetics and molecular docking studies of kaempferol and its prenylated derivatives as aldose reductase inhibitors, Chemico-Biol. Interact. 197 (2–3) (2012) 110–118, https://doi.org/10.1016/j.cbi.2012.04.004. PMID: 22543015.

[7] Y. Dong, H. Huang, M. Zhao, D. Sun-Waterhouse, L. Lin, C. Xiao, Mechanisms underlying the xanthine oxidase inhibitory effects of dietary flavonoids galangin and pinobanksin, J. Funct. Foods 24 (2016) 26–36, https://doi.org/10.1016/j.jff.2016.03.021.

[8] S. Lin, G. Zhang, Y. Liao, J. Pan, Inhibition of chrysin on xanthine oxidase activity and its inhibition mechanism, Int. J. Biol. Macromol. 81 (2015) 274–282, https://doi.org/10.1016/j.ijbiomac.2015.08.017. PMID: 26275460.

[9] F. Rasoulzadeh, H.N. Jabary, A. Naseri, M.R. Rashidi, Fluorescence quenching study of quercetin interaction with bovine milk xanthine oxidase, Spectrochim. Acta. Part A, Mol. Biomol. Spectros. 72 (1) (2009) 190–193, https://doi.org/10.1016/j.saa.2008.09.021. PMID: 19028136.

[10] S. Lin, G. Zhang, Y. Liao, J. Pan, D. Gong, Dietary flavonoids as xanthine oxidase inhibitors: structure-affinity and structure-activity relationships, J. Agric Food Chem. 63 (35) (2015) 7784–7794, https://doi.org/10.1021/acs.jafc.5b03386. PMID: 26285120.

[11] J. Yan, G. Zhang, Y. Hu, Y. Ma, Effect of luteolin on xanthine oxidase: inhibition kinetics and interaction mechanism merging with docking simulation, Food Chem. 141 (4) (2013) 2766–2773, https://doi.org/10.1016/j.foodchem.2013.06.092. PMID: 23993547.

[12] M.D. Santi, M. Paulino Zunini, B. Vera, C. Bouzidi, V. Dumontet, A. Abin-Carriquiry, R. Grougnet, M.G. Ortega, Xanthine oxidase inhibitory activity of natural and hemisynthetic flavonoids from Gardenia Oudiepe (Rubiaceae) in vitro and molecular docking studies, Eur. J. Med. Chem. 143 (2018) 577–582, https://doi.org/10.1016/j.ejmech.2017.11.071. PMID: 29207340.

[13] P. Jayaraj, B. Mathew, B. Parimaladevi, V.A. Ramani, R. Govindarajan, Isolation of a bioactive flavonoid from Spilanthes Calva D.C. in vitro xanthine oxidase assay and in Silico study, Biomed. Prevent Nutr. 4 (4) (2014) 481–484, https://doi.org/10.1016/j.bionut.2014.07.005.

[14] C.E. Cassidy, W.N. Setzer, Cancer-relevant biochemical targets of cytotoxic lonchocarpus flavonoids: a molecular docking analysis, J. Mol. Model. 16 (2) (2010) 311–326, https://doi.org/10.1007/s00894-009-0547-5. PMID: 19603203.

[15] M.A. Peralta, M.D. Santi, J.L. Cabrera, M.G. Ortega, Dalea Genus, Chemistry, and Bioactivity Studies, in: Studies in Natural Products Chemistry, 62, Elsevier B.V, 2019, pp. 307–341, https://doi.org/10.1016/B978-0-444-64185-4.00008-3.

[16] M.D. Santi, F. Arredondo, D. Carvalho, C. Echeverry, G. Prunell, M.A. Peralta, J. L. Cabrera, M.G. Ortega, E. Savio, J.A. Abin-Carriquiry, Neuroprotective effects of prenylated flavanones isolated from Dalea species, in vitro and in silico studies, Eur. J. Med. Chem. (2020) 206, https://doi.org/10.1016/j.ejmech.2020.112718.

[17] M. Caffaratti, M.G. Ortega, M.E. Scarafia, L. Ariza Espinar, H.R. Juliani, Prenylated flavanones from Dalea elegans, Phytochemistry 36 (4) (1994) 1082–1084.

[18] M.A. Peralta, M.G. Ortega, A.M. Agnese, J.L. Cabrera, Prenylated flavanones with anti-tyrosinase activity from Dalea Boliviana, J. Nat. Prod. 74 (2) (2011) 158–162, https://doi.org/10.1021/np1004664. PMID: 21226489.

[19] M.A. Peralta, M.D. Santi, A.M. Agnese, J.L. Cabrera, M.G. Ortega, Flavanoids from Dalea elegans: chemical reassignment and determination of kinetics parameters related to their anti-tyrosinase activity, Phytochem. Lett. 10 (2014) 260–267, https://doi.org/10.1016/j.phytol.2014.10.012.

[20] M.D. Santi, M.A. Peralta, C.S. Mendoza, J.L. Cabrera, M.G. Ortega, Chemical and bioactivity of flavanones obtained from roots of Dalea Pazensis Rusby, Bioorg. Med. Chem. Lett 27 (8) (2017) 1789–1794, https://doi.org/10.1016/j.bmcl.2017.02.058. PMID: 28268138.

[21] G. Schmeda-Hirschmann, J.I. Loyola, J. Sierra, R. Retamal, J. Rodriguez, Hypotensive effect and enzyme inhibition activity of mapuche medicinal plant extracts, Hypotensive Effect and Enzyme Inhibition Activity of Mapuche Medicinal Plant Extracts 6 (4) (1992) 184–188.

[22] Strelow, J.; Dewe, W.; Iversen, P. W.; Brooks, H. B.; Radding, J. A.; McGee, J.; Weidner, J. Mechanism of Action Assays for Enzymes; 2004.

[23] Kuzmic, P. Optimal Duration of the Preincubation Phase in Enzyme Inhibition Experiments, 2020. http://www.biokin.com. (accessed 2023-09-06).

[24] Rodrigues, A. David. Drug-Drug Interactions; Informa Healthcare, 2008.

[25] H. Bisswanger, Enzyme assays, Perspect. Sci. (Neth) 1 (1–6) (2014) 41–55, https://doi.org/10.1016/j.pisc.2014.02.005.

[26] H.M. Berman, J. Westbrook, Z. Feng, G. Gilliland, T.N. Bhat, H. Weissig, I. N. Shindyalov, P.E. Bourne, The Protein Data Bank 28 (2000) 235–242. http://www.rcsb.org/pdb/status.html.

[27] Molecular Operating Environment (MOE) 2015.10, Chemical Computing Group Inc., 1010 Sherbooke St. West, Suite #910, Montreal, QC, Canada, H3A 2R7 (2015).

[28] Halgren, T. A. MMFF VI. MMFF94s Option for Energy Minimization Studies. J Comput Chem 1999, 20 (7). 720-729.

[29] M.P. Allen, D.J. Tildesley, Computer Simulation of Liquids, 2nd ed., Clarendom Press, New York, 1987.

[30] P. Labute, LowModeMD - Implicit low-mode velocity filtering applied to conformational search of macrocycles and protein loops, J. Chem. Inf. Model. 50 (5) (2010) 792–800, https://doi.org/10.1021/ci900508k. PMID: 20429574.

[31] E. Alvareda, P. Miranda, V. Espinosa, H. Pardo, S. Aguilera, M. Paulino Zunini, 196 Antiinflamatory activity of phenolic compounds extracted from uruguayan propolis and grape, J. Biomol. Struct. Dyn. 33 (sup1) (2015) 129, https://doi.org/10.1080/07391102.2015.1032833.

[32] Paulino Zunini, M.; Alvareda, E.; Iribarne, F.; Miranda, P.; Espinosa, V.; S. Aguilera, S.; Pardo, H. Anti-inflammatory Activity of Phenolic Compounds extracted from Uruguayan Propolis and Grape (Vitis vinifera) Pomace: In Vitro and In Silico Assays, J. Biomol. Struct. Dyn. 2016, 34, 2643-2657. M. Paulino, E. Alvareda, F. Iribarne, P. Miranda, V. Espinosa, S. Aguilera, H. Pardo, Anti-inflammatory Activity of Phenolic Compounds extracted from Uruguayan Propolis and Grape (Vitis vinifera) Pomace: In Vitro and In Silico Assays, J. Biomol. Struct. Dyn. 34 (2016) 2643-2657.

[33] H. Cao, J.M. Pauff, R. Hille, X-ray crystal structure of a xanthine oxidase complex with the flavonoid inhibitor quercetin, J. Nat. Prod 77 (7) (2014) 1693–1699, https://doi.org/10.1021/np500320g. PMID: 25060641.

[34] N. Malik, P. Dhiman, A. Khatkar, In silico design and synthesis of hesperitin derivatives as new xanthine oxidase inhibitors, BMC Chem (2019) 13, https://doi.org/10.1186/s13065-019-0571-1.

[35] A. Mehmood, M. Ishaq, L. Zhao, B. Safdar, A.-u. Rehman, M. Munir, A. Raza, M. Nadeem, W. Iqbal, C. Wang, Natural compounds with xanthine oxidase inhibitory activity: A review, Chem. Biol. Drug Des. 93 (4) (2019) 387–418.

[36] H. Tamta, R. Thilagavathi, A.K. Chakraborti, A.K. Mukhopadhyay, 6-(N-Benzoylamino)purine as a novel and potent inhibitor of xanthine oxidase: inhibition mechanism and molecular modeling studies, Med. Chem. 20 (4) (2005) 317–324, https://doi.org/10.1080/14756360500112326. PMID: 16206825.

[37] S. Floris, A. Fais, A. Rosa, A. Piras, H. Marzouki, R. Medda, A.M. González-Paramás, A. Kumar, C. Santos-Buelga, B. Era, Phytochemical composition and the cholinesterase and xanthine oxidase inhibitory properties of seed extracts from the: Washingtonia Filifera Palm fruit, RSC Advances 9 (37) (2019) 21278–21287, https://doi.org/10.1039/c9ra02928a.

[38] M. Kaur, A. Kaur, S. Mankotia, H. Singh, A. Singh, J.V. Singh, M.K. Gupta, S. Sharma, K. Nepali, P.M.S. Bedi, Synthesis, screening and docking of fused pyrano [3,2-d]pyrimidine derivatives as xanthine oxidase inhibitor, Eur. J. Med. Chem. 131 (2017) 14–28, https://doi.org/10.1016/j.ejmech.2017.03.002. PMID: 28286211.